ACTA MECHANÌCA ET MOBILITATEM
Vol. 2 – 2017
2017-05-100

ADJUSTABLE STROKE LENGTH AND COMPRESSION RATIO ENGINE

C. H. Rufino[a],
and J. V. Ferreira[a]

[a] Universidade Estadual de Caminas- Brazil
Contact Information
rufino119186@gmail.com.

ABSTRACT

Recently, research on internal combustion engines for the automobile industry aims the increase of efficiency. The main motivation is the environmental regulations, which are being adjusted to force an urgent reduction in the vehicular emission of pollutants. Among the technologies in development that bring an increase in the efficiency of engines, it can be highlighted the strategies used to adjust the compression ratio according to the operational requirements of the engine. Another strategy is to reduce the opening/closing of the throttle valve to limit the output power by adopting an alternative, being by means of adjusting the valve synchronism or by means of varying the stroke length and thus varying the cubic capacity, resulting in the maintenance of a higher pressure in the intake manifold and avoiding the negative pump work. This work presents a mechanism that allows the adjustment of both compression ratio and stroke length. Therefore, the engine can operate at partial loads without restricting the flow to the intake manifold and the compression ratio can vary to obtain a higher efficiency when there is no risk of the knock to occur and also, it is possible to guarantee a better adaptability, fundamental requirement for a multi-fuel engine. The proposed engine is described, showing and explaining the strategy adopted and, following, a preliminary study made by computational simulation is presented, illustrating and justifying how the technology has the potential to increase the efficiency of spark ignition engines.

Keywords: Variable compression ratio, Spark ignition engines, Zero-dimensional simulation

NOMENCLATURE

A area of the cylinder, m²
A_i area of flow through valves
C_D Coefficient of discharge, nondimensional
C_m piston's mean velocity, m/s²
Cp specific heat at constant pressure, J/(kgK)
Cv specific heat at constant volume, J/(kgK)
D_c diameter of the cylinder, m
h coefficient of heat transfer, W/(m²K)
IMEP indicated mean effective pressure, bar
k specific heat ratio, nondimensional
LHV lower heating value, J/kg
m_0 theoretical in-cylinder mass of gasses, kg
m_c in-cylinder mass of gasses, kg
m_{comb} mass of fuel, kg
m_i mass of gasses flowed through valves, kg
$\dot{m}_i$ mass flow through valves, kg/s
m_{total} total mass of gasses flowed into the cylinder, kg
m_w Wiebe's function parameter of shape, nondimensional
P in-cylinder pressure, Pa
P_0 atmospheric pressure, Pa
R gasses constant, J/(kgK)
S/D stroke/diameter ratio, nondimensional
sfc specific fuel consumption, g/kWh
T in-cylinder temperature, K
T_0 atmospheric temperature, K
T_w temperature of the cylinder wall, K
V instantaneous volume of the cylinder, m³
V_{max} maximum volume of the cylinder, m³
$\dot{W}$ net power output, kW
W_{Cycle} work developed in the cycle, J
X_b fraction of burnt fuel, nondimensional

Greek symbols

$\Delta\theta_b$ combustion duration, °
η_{comb} combustion efficiency, nondimensional
$\eta_{comb,m}$ maximum efficiency of combustion, nondimensional
η_r maximum fraction of burnt fuel, nondimensional
η_T thermal efficiency, nondimensional
η_V volumetric efficiency, nondimensional
θ crank position, °

θ_0	combustion start, °
λ	relative air/fuel ratio, nondimensional
ω	angular velocity of the engine, rad/s

Subscripts

ds	downstream
ex	exhaust
in	intake
mixt	air-fuel mixture
prod	products of combustion
us	upstream

INTRODUCTION

Environmental research has proven the urgent necessity of the development of alternative technology for energy production and utilization in order to reduce the pollutant and GHG. Among the many technological sectors, the automotive sector is one of the greatest contributors to the emission of pollutants to the atmosphere. For instance, urban vehicles are estimated to be responsible for 30% of the emissions in the USA [1]. With the objective to change this scenario, public organs has started to establish limits to vehicular emission, impacting directly in the development of the automobile industry. The European Committee has created the Euro standard of emission, recently the phase VI, whose objective is to impose reduction goals for pollutant emissions seeking a health improvement. Similarly, the Environment Protection Agency (EPA) of USA has implemented a program of control on emissions of green house effect gasses [2]. In the Brazilian scenario, the Proconve program has been implemented in 1986, recently in its phase V, which initial goal was to promote the investment in technology in the automobile industry and thus guarantee the adequate maintenance, fundamental for emission control, provided by the user [3]. More recently, another Brazilian program has incentivized the research on technology for improvement of energetic efficiency of vehicles and as a consequence the reduction on pollutant emission, which is nominated as Inovar-Auto [4], foreseeing the taxes reduction for the factories compromised with the goals imposed by the program until 2017.

There are promising alternatives for the internal combustion engine, such as electrical engine, fuel cell, and hybrid system, however, those are considered long term solution for the reduction of pollutant emission and, in some cases highly dependent on other sources of energy, so it is desirable to keep the research on more efficient internal combustion engines in parallel to the development of those technologies [5]. Among the strategies adopted nowadays to improve efficiency of engines can be cited: downsizing, direct injection and control over the opening and lifting of valves. Other strategies can be more audacious since it is required the redesign of components, as variable compression ratio and variable stroke engines, which are still in phase of development, present a viable proposal for high efficiency, multifuel engines in the middle term.

The challenge in the project of urban vehicles is the variability of the operational conditions in which the automobile will be exposed during its lifetime, generated by traffic in urban transportation, making difficult the design of the engines. To overcome this issue, it is necessary to improve the flexibility of engine by adjusting its parameters which were firstly fixed, allowing the engine to adapt itself to the situation in which one is operating or to allow the use of alternative fuels, stating that each fuel require different conditions for an optimized function of the engine. The multifuel engine was introduced in Brazil in 2003, which could operate with gasoline or hydrous ethanol or a mixture of both fuels at any concentration and the selling of this type of engine has reached 80% of all vehicles sold in Brazil from 2009 [6]. The drawback of such technology is the need of a constant compression ratio, usually chosen to be the intermediate of the ideal compression ratio for each fuel. The gasoline has a higher sensibility to knock, requiring a lower compression ratio while not only an air-ethanol mixture can be compressed to a higher compression ratio without knocking, but it is desired to do so in order to obtain a higher efficiency of combustion. Therefore, when the intermediate compression ratio is chosen, the engine will operate at a lower efficiency with ethanol and also it will be necessary to compensate the high compression ratio for the gasoline by the delay of the spark to avoid knock, which also reduces efficiency.

Variable Compression Ratio (VCR) engines allow to control compression ratio at real time. This adjustment is convenient once the compression ratio of a conventional engine is defined for the conditions in which the engine is near its critical condition for knock, i.e., the conditions in which self-ignition of the air-fuel mixture is favoured by the historic of temperature and pressure of the mixture and ignition occurs, reaching supersonic conditions and producing acoustic waves that harm the engine. These critical conditions occurs at low speed and full load, when the in-cylinder pressure is higher, which is attained only at a few moments during the use of the vehicle. Therefore, at most time the engine is far from the conditions of knock and thus it would be possible to increase he compression ratio to obtain a better efficiency [7] and [8], what will be shown ahead in this work. Several arrangement have been proposed in the literature, citing: variable geometry of the combustion chamber [9], moving head [10], eccentric connecting rod pin [11], adjustable head height piston [12], multi-link mechanism [7], adjustable top dead centre [13], eccentric crank pin [8].

Other mechanisms go beyond the adjustment of the compression ratio and also permit the variation of the stroke length, nominated Variable Stroke Engines

(VSE). VSE engines propose the reduction of stroke length seeking a limitation of the power output due to the reduction of the cubic capacity. By this mean, it is possible to limit the actuation of the throttle valve, avoiding the pump losses that appear when the pressure in the intake manifold is restrained by the throttle, resulting that the engine will operate at conditions near of those when it is operating at full load. This type of engine has been researched since the beginning of the use of spark ignition engines [14], but the redesign needed for its implementation has delayed its development. Also, studies are required for this engine since the reduction of the stroke length can cause some inconvenience such as the delayed flame front and the increasing of the area/volume ratio, which increases losses due to heat transfer [15]. However, other studies have shown that the gain in volumetric efficiency compensates the cited losses and the VSE could still bring advantages over the conventional engines. Among the proposals, can be cited the Mayflower e-3 engine [7], Pouliot's engine [16], Rosso and Beard [17] and Freudenstein and Maki [18]. The importance of the mechanism having three degrees of freedom can be highlighted, being one degree of freedom related to the motion of the crank, and the other two used to control the compression ratio and the stroke length independently. An exception is given by an European patent [19], in which the compression ratio is kept low at high cubic capacity, what is questionable as a convenient strategy.

The object of study in this work consists in a VSE muli-link mechanism with three degrees of freedom, which was patented in the INPI in 2014 [20] since it is characterized by an innovative solution. Following it is presented the description of the mechanism and the explanation of its functioning, the description of the model of simulation, used to simulate and predict the performance of the engine operating with the proposal. Afterwards results, discussion on the presented results and conclusions are presented.

THE MECHANISM

The proposal consists in including a lever between piston and connecting rod. The crank-rod system converts the alternative motion of the piston-lever in the rotative motion of the shaft. Thus, it is necessary to pin one of the ends of the lever to a rod, connected to the piston while the other end is fixed by a pivot, which allows only the lever to slide in that point. The connecting rod is pinned between pivot and piston rod. By these means, the kinematics of the piston depends on the position of the pivot. The top dead centre is altered when the pivot moves upwards or downwards, increasing and decreasing the volume of combustion chamber, respectively, and therefore, decreasing or increasing compression ratio. By moving the pivot in the horizontal position it is possible to modify the length of one side of the lever and as result the stroke length changes. As the connecting rod is connected to the central portion of the lever, the convenient nature of the crank-rod motion is preserved (slow velocity of the piston at top dead centre and higher velocity at bottom dead centre).

Figure (1) shows a conception of the mechanism with one alternative to control the position of the pivot. One can note that this set is composed by two hydraulic actuators, which is only one of several means by which it is possible to perform the control on the position of the pivot. The fact that the piston rod can absorb the forces generated by the motion of the lever and connecting rod is highlighted since it reduces the lateral forces actuating in the head of the piston.

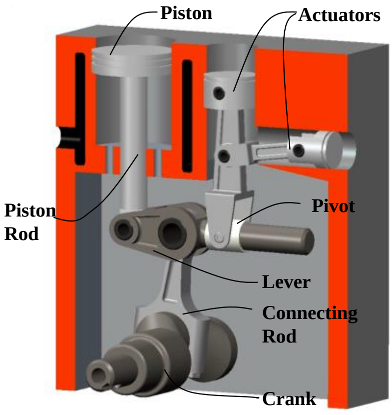

Figure 1. Model of the mechanism.

In order to simulate functioning of an engine composed by mechanism, it had been necessary to map the piston kinematics as function of the position of the pivot (relative to the shaft) and then to determine the characteristics (compression ratio, cubic capacity, stroke/diameter ratio and stroke length) as function of the kinematics of the piston. Compression ratio and stroke length are demonstrated graphically by Figures (2) and (3), respectively.

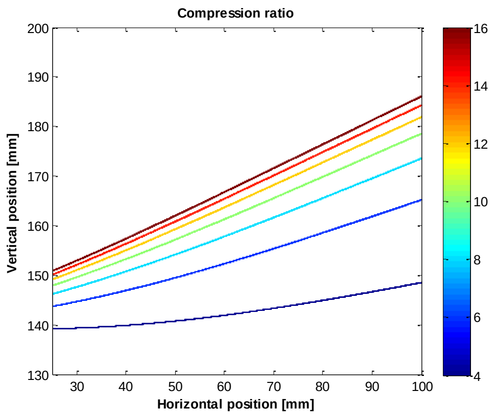

Figure 2. Compression ratio map.

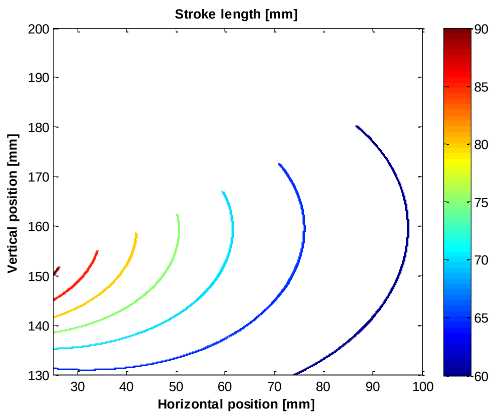

Figure 3. Stroke length map.

Setting the diameter of the cylinder to 77.6 mm, the cubic capacity can be determined as a function of the stroke length, as shown by Figure (4):

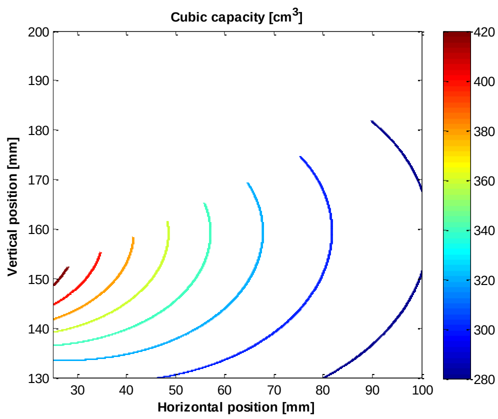

Figure 4. Cubic capacity map.

Another relevant factor is the stroke/diameter ratio of the engine. Engines with a low stroke/diameter ratio (**S/D**<<1) have a high area/volume ratio, which can be an advantage in terms of torque, however, it is undesired when a high efficiency is required, since the area/volume ratio affects the amount of losses by heat transfer [15]. Figure (5) shows the **S/D** ratio in which the proposed engine operates at each condition, leading to a lowest **S/D** ratio of 0.75.

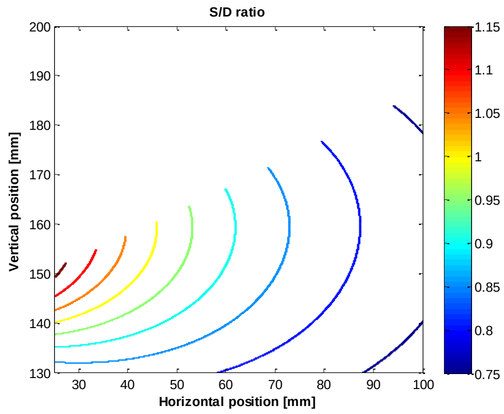

Figure 5. **S/D** ratio map

SIMULATION MODEL

To predict the performance of the proposed engine, a thermodynamic (or phenomenological) model with one zone of combustion was developed. In the simulation there are two unknown variables, in-cylinder temperature **T** and in-cylinder pressure **P**. The thermodynamic model consists in the application of the balance of energy and state equations in each of the six phases of the thermodynamic cycle, being three closed phases and three open phases: induction, combustion and power composing the closed phase and the open phase composed by: exhaust, valve overlapping (in which exhaust occurs simultaneously with intake) and intake. Before the thermodynamic analysis, a kinematics analysis is performed, obtaining the instantaneous volume **V** and its rate **dV/dθ** and also the instantaneous area of the cylinder **A**, parameter that will be used by the thermodynamic model.

By performing the balance of energy in its differential form (first law of thermodynamic) it is possible to obtain the differential of temperature related to the crank position **θ**:

$$\frac{dT}{d\theta} = \left[m_c \left(Cv_{mixt} + T \frac{\partial Cv_{mixt}}{\partial T} \right) \right]^{-1} \left[\eta_{comb} m_{comb} LHV \frac{dX_b}{d\theta} - \frac{hA(T - T_w)}{\omega} - P \frac{dV}{d\theta} + \left(Cp_{us,ex} T_{us,ex} - Cv_{mixt} T \right) \frac{dm_{ex}}{d\theta} + \left(Cp_{us,in} T_{us,in} - Cv_{mixt} T \right) \frac{dm_{in}}{d\theta} \right] \quad (1)$$

The denominator of Eq. (1) refers to the internal energy of the mixture of in-cylinder gasses due to variation of temperature, in which $\mathbf{m_c}$ represents the mass of gasses in the cylinder. Specific heats of the air-fuel mixture $\mathbf{Cv_{mixt}}$ e $\mathbf{Cp_{mixt}}$ are adjusted by polynomial interpolation using tables of thermodynamic data [21]. Once the functions are determined, it is easy to obtain the partial derivative of the specific heat $\partial Cv_{mixt}/\partial T$.

The term $\eta_{comb} m_{comb} LHV dXb/d\theta$ is related to the heat liberated by combustion. The mass of fuel m_{comb} is determined by the stoichiometry of the mixture, given by relative air-fuel ratio λ. **LHV** is the lower heating value of the fuel and the rate of burning is given by a function $dX_b/d\theta$, which in this case is modelled by Wiebe function, the start of combustion is given by θ_0 and duration of the combustion is given by $\Delta\theta_b$, as shown by Eq. (2) [22]:

$$X_b = 1 - \exp\left[(1-\eta_r)\left(\frac{\theta-\theta_0}{\Delta\theta_b}\right)^{m_w+1}\right] \quad (2)$$

in which η_r is the maximum fraction of burnt fuel, while factor m_w defines the shape of the burning profile. The amount of energy liberated by combustion as heat is given by the efficiency of combustion η_{comb}, given by Eq. (3) as a function of stoichiometry [23]:

$$\eta_{comb} = \eta_{comb,m}\left(-1.6082 + 4.6509\lambda - 2.0764\lambda^2\right) \quad (3)$$

The term $hA(T - T_w)/\omega$ models heat transfer by convection through walls of cylinder, which is assumed to be constant T_w. It is stated that the law of convection $hA\Delta T$ gives the heat transfer in means of time, but the differential equations used in the model are given by means of crank position, so it is necessary to perform a transformation by dividing the term by ω. The heat transfer coefficient **h** is given by semi-empirical correlations available in the literature, using the model proposed by Hohenberg [24] for the closed phases (Eq. (4)) and the model proposed by Nishiwaki [25] (Eqs. (5) e (6)) for the open phases. The choice of those models was made based on the reliability and simplicity of those models.

$$h = 130 V^{-0.06} P^{0.8} T^{-0.4} (C_m + 1.4)^{0.8} \quad (4)$$

$$h = 82.3 D_c^{-0.193} (C_m P)^{0.807} T^{-0.534} \quad (5)$$

$$h = 679 D_c^{-0.422} (C_m P)^{0.578} T^{-0.199} \quad (6)$$

in which C_m is the mean velocity of piston and D_c is the diameter of the cylinder. The equation related to the heat transfer during intake is Eq. (6) while the one related to the exhaust is Eq. (5).

The work done by the piston is given by $PdV/d\theta$. From this amount of work, a portion is transferred to the atmosphere, while the rest is transferred to the shaft to produce power output of the engine.

The effects of mass transport in the balance of energy is given by the terms $(Cp_{us,i}T_{us,i} - Cv_{mixt}T)dmi/d\theta$ being the subscript **i** related to the origin or destiny of the gasses, being **in** to intake manifold or **ex** for exhaust manifold. The increase of energy given by the transferred mass is given by the enthalpy of the gasses in the upstream conditions $Cp_{us,i}T_{us,i}dm_i/d\theta$, being **us** the subscript of upstream conditions. The variation of internal energy induced by the mass flow is given by $Cv_{mixt}Tdm_i/d\theta$. As the described model does not consider the blow-by phenomenon there is no mass transportation during the closed phases. To determine the mass flow through any valve $\dot{m}_i$, it is used the quasi-steady model, which considers the isoentropic flow at steady conditions, corrected by a coefficient of discharge C_D, given by the interpolation of experimental data as a function of the valve lift, proposed by Kastner [26] and revised by Gallo [27].

Equation (7) gives the criteria to the choked flow.

$$\frac{P_{ds}}{P_{us}} \le \left(\frac{2}{k+1}\right)^{\frac{k}{k-1}} \quad (7)$$

In the case of choked, or sonic, the flow is function of the conditions upstream (Eq. (8)), while in the subsonic flow, the conditions at downstream also have influence on mass flow (Eq. (9)).

$$\dot{m}_i = C_D \frac{A_i P_{us}}{\sqrt{RT_{us}}} \sqrt{k\left(\frac{2}{k+1}\right)^{\frac{k+1}{k-1}}} \quad (8)$$

$$\dot{m}_i = C_D \frac{A_i P_{us}}{RT_{us}} \sqrt{2\left(\frac{k}{k-1}\right)\left[\left(\frac{P_{ds}}{P_{us}}\right)^{\frac{2}{k}} - \left(\frac{P_{ds}}{P_{us}}\right)^{\frac{k+1}{k}}\right]} \quad (9)$$

In the presented relations, **k** is the specific heat ratio and **R** is the gas constant of the flowed gas. The area of flow A_i is given by means of the valve lift and geometry.

Once the temperature differential is determined, it is possible to obtain the pressure differential by using an equation of state. Although the pressure in the cylinder can attain elevated values, the partial pressure of each component of the mixture is lower and the temperature is high enough to the ideal gas hypothesis to be reasonable [28]. The differential form of the ideal gasses relation is given by Equation (10).

$$\frac{dP}{d\theta} = P\left(\frac{dm_{total}}{d\theta}\frac{1}{m_c} + \frac{dT}{d\theta}\frac{1}{T} - \frac{dV}{d\theta}\frac{1}{V}\right) \quad (10)$$

in which it has been neglected the variation of the constant of gasses **$dR/d\theta$**.

Given the differentials of temperature and pressure, a numerical integration is implemented. The initial values of the variables (pressure, temperature and mass of gasses at the end of the intake) are given at first iteration by ambient conditions (**P_0**, **T_0** e **m_0**). At the beginning of each of the following iterations, initial values are updated with final value of the previous iteration until the difference between values obtained in the previous iteration and the last iteration are within an imposed tolerance (chosen to be 0,1% of calculated parameters). The numeric method used was the Runge-Kutta of 5th order, also known as Butcher method [29].

Being the thermodynamic properties of the cycle determined, the performance parameters to be analysed can be calculated. In this work it was decided to perform an energetic analysis (irreversibilities effects were not considered), gathering information of indicated power **$\dot{W}$** (Eq. (12)), thermal efficiency **η_T** (Eq. (13)), volumetric efficiency **η_V** (Eq. (14)), indicated mean effective pressure **IMEP** (Eq. (15)) and specific fuel consumption **sfc** (Eq. (16)). Since the mechanism is different from the conventional and the friction model is given for conventional engines, it was decided to neglect effects of friction.

Work done in a cycle **W_{Cycle}** is given by:

$$W_{Cycle} = \int (P - P_0)dV \quad (11)$$

With work done in one cycle, indicated power is given by the product of angular velocity and work:

$$\dot{W} = W_{Cycle}\frac{\omega}{2} \quad (12)$$

Thermal efficiency is given by the ratio between work produced in a cycle **W_{Cycle}** and energy given by the fuel, which is the product between mass of fuel **m_{comb}** and lower heating value **LHV**:

$$\eta_T = \frac{W_{Cycle}}{m_{comb}LHV} \quad (13)$$

Volumetric efficiency is given by the ratio between mass admitted in the cylinder **m_c** and maximum of mass that would be admitted in ideal conditions **m_0**:

$$\eta_V = \frac{m_c}{m_0} \quad (14)$$

Indicated mean effective pressure is a measure of power density produced by the engine. Its definition is given by the equivalent constant pressure in which the same work would be developed by the real in-cylinder pressure profile. To calculate this parameter work developed in the cycle is divided by displaced volume in the cylinder **V_{max}**:

$$IMEP = \frac{W_{Cycle}}{V_{max}} \quad (15)$$

Specific fuel consumption is defined by the amount of fuel consumed to generate a certain amount of energy, i.e., it is the mass of fuel **m_{comb}** divided by work developed in one cycle **W_{Cycle}**:

$$sfc = \frac{m_{comb}}{W_{Cycle}} \quad (16)$$

RESULTS AND DISCUSSION

Simulations were performed for the mechanism presented in Figure (1). The fuel considered in the simulation was anhydrous ethanol and other parameters related to the geometry of the engine and conditions of operation are given in Table 1:

Table 1. Simulation parameters

Parameter	Value
Atmospheric pressure	101,325 Pa
Atmospheric temperature	298.15 K
Diameter of the cylinder	77.6 mm
Valves per cylinder	2
Intake V. (diameter/lift)	30.93/9.28 mm
Exhaust V. (diameter/lift)	28.27/8.48 mm
Intake duration	230°
Exhaust duration	245°
Intake valve opening	340°
Exhaust valve opening	130°
Engine speed	3,000 rpm
Pressure in the intake manifold	86,000 Pa
Pressure in the exhaust manifold	115,000 Pa
Temperature of the cylinder wall	520 K
Spark time	-20°
λ	1

The following results were obtained with the engine operating at a constant cubic capacity of 400 cm^3, full load and compression ratio from 8:1 to 16:1.

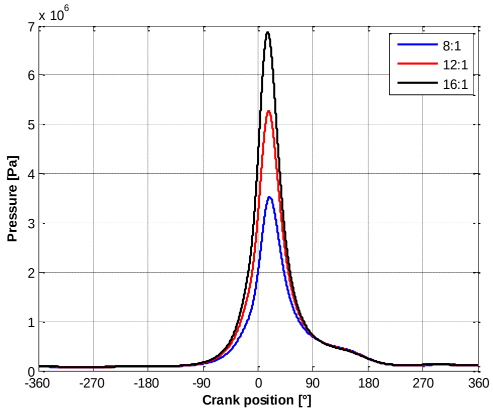

Figure 6. In-cylinder pressure

Figure (6) shows how compression strongly affects the in-cylinder pressure peak. The outcome of that rise in pressure peak is a gain in thermal efficiency, as shown in Fig. (7).

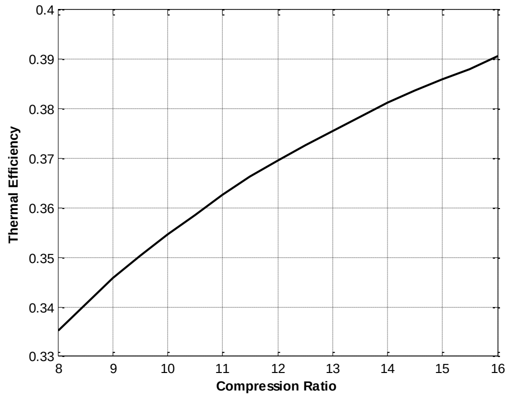

Figure 7. Influence of the compression ratio on the thermal efficiency.

Other phenomena that are not considered in the simulation could collaborate to the increase of efficiency, such as combustion efficiency and flame velocity. Also, higher compression ratio produces a more complete combustion, which reduces emission of unburnt hydrocarbons and intermediate products of combustion. The only phenomenon limiting the compression ratio is the knock phenomena, which is critical, as mentioned before [7].

In the conditions covered in the test it was not observed a significant increase in the indicated power. This conclusion is illustrated by Fig. (8) which presents a gain of only 2 bar in a large variation of 8:1 to 16:1 in compression ratio.

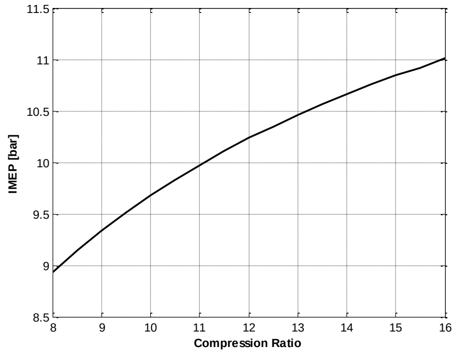

Figure 8. Influence of the compression ratio on the IMEP

Figure (9) also presents a weak correlation between compression ratio and volumetric efficiency, giving an increasing of only 0.2% within the range tested. This gain is probably result of the reduced dead volume, what reduces the residual amount of burnt gasses, allowing a greater amount of fresh air-fuel mixture to be admitted in the cylinder.

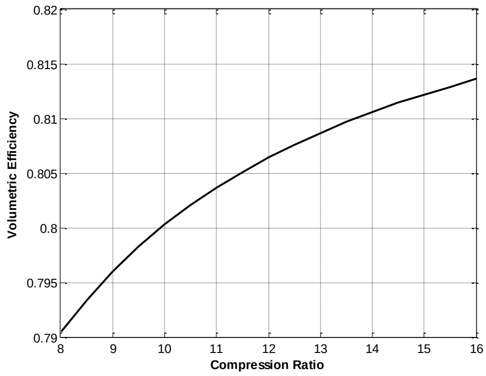

Figure 9. Influence of the compression ratio on the volumetric efficiency

As fuel consumption is directly correlated to thermal efficiency, it is expected to obtain a reduction in specific fuel consumption, as it was proven by Fig. (10).

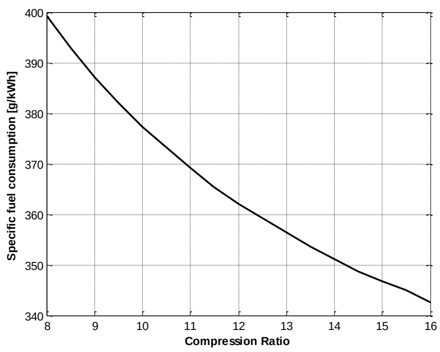

Figure 10. Influence of the compression ratio on the specific fuel consumption

Therefore, as compression ratio is increased, the obtained results indicate that it is expected to the engine to develop the same indicated power, but since thermal efficiency increases, fuel consumption is reduced.

Figure (11) presents the Pressure-Volume diagram to three compression ratio values. Besides the pressure rising, it is noted the reduction of dead volume (minimum volume), necessary condition to execute the compression ratio increasing, what can be verified by the dislocation of the curves to the left in the diagram.

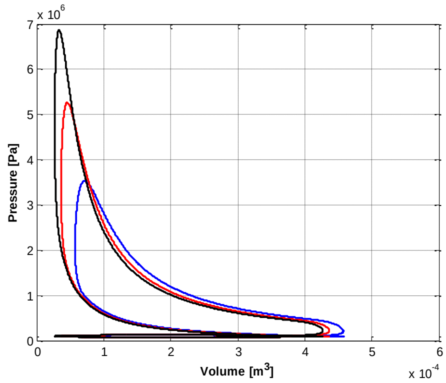

Figure 11. Pressure-volume diagram for variation of compression ratio

Another simulation was performed varying load between 60% and 100% (full load), and keeping a constant cubic capacity of 400 cm³ and a constant compression ratio of 12:1. The reduction of load is understood as the pressure reduction in the intake manifold, since throttle opening has a strongly non-linear relation to that parameter. As pressure in intake manifold is reduced, a smaller amount of gasses is admitted in the cylinder, (Fig. (12)), and as results, the indicated power will be limited (Fig. (13)). The inconvenience of this practice is the additional pump work generated by the reduction in intake pressure, as it was mentioned before. Consequently, part of the power produced by the engine is used to pump gasses inside the cylinder.

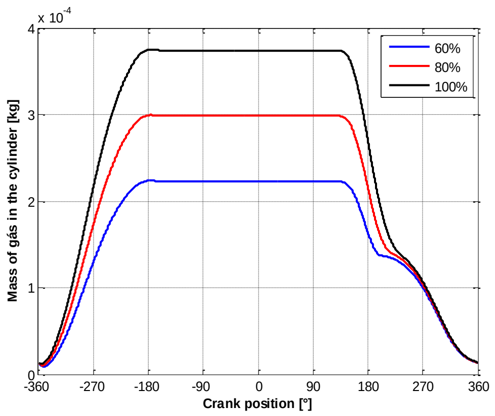

Figure 12. In-cylinder mass of gasses for variation of load.

At Figure (12) it can be perceived the backflow phenomenon at the end of the intake process, when part of the admitted gasses flow back to the intake manifold, observed by a peak of mass that is located near -180° of crank position. In the same figure it is shown the process of exhaust. Before bottom dead centre (180°), gasses are expelled from the cylinder by the elevated pressure of the same, and after bottom dead centre, the gasses are expelled by the motion of piston, which can be seen by an inflexion in the curve after 180°.

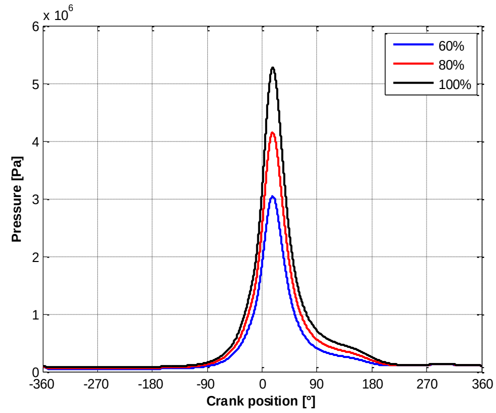

Figure 13. In-cylinder pressure for variation of load

Figure (14) presents the P-V diagrams for three conditions of load.

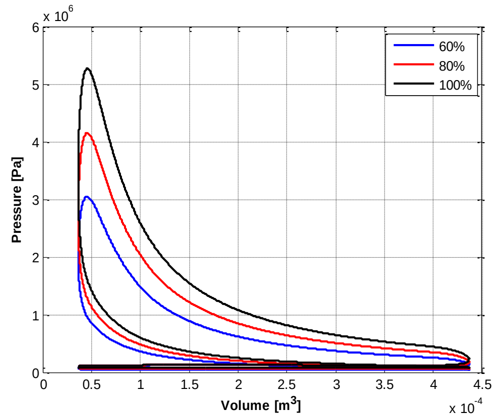

Figure 14. Pressure-volume diagram for variation of load

By detailing the open processes, Figure (15) shows the reduction in intake pressure at partial loads. One can note that this process occurs at a pressure that is inferior to atmospheric pressure, meaning that the work done by the piston is negative (work is done to the cylinder), which is numerically given by the area between atmospheric pressure (101,325 kPa) and intake pressure. As the load is decreased, the area between atmospheric pressure and intake pressure will increase, and therefore, the greater will be the negative work.

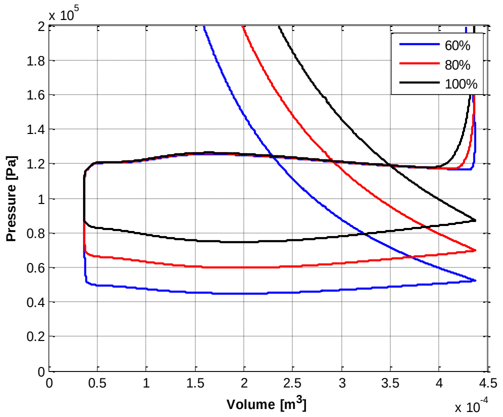

Figure 15. Detail of the open processes on the P-V diagram for variation of load

In parallel to the simulation in which the load was varied, it was made a simulation varying the cubic capacity from 300 cm³ to 400 cm³, keeping compression ratio constant at 12:1 and full load. This strategy aims to restrict the power output without harming the volumetric efficiency, without reducing intake pressure and, thus, avoiding negative work. Therefore, load is kept at its full value while stroke length is reduced. By those means it is also admitted a smaller amount of gasses in the cylinder, as shown by Fig. (16).

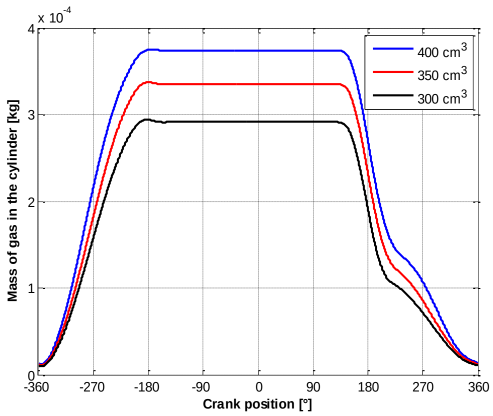

Figure 16. In-cylinder mass of gasses for variation of cubic capacity.

However, in the P-V diagram (Fig. (17)) it is observed that the pressure is kept practically constant, except for a sensible reduction in the pressure peak at higher cubic capacities.

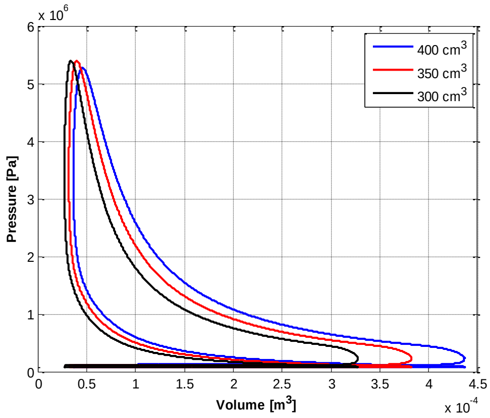

Figure 17. Pressure-volume diagram for variation of cubic capacity.

Figure (17) above also presents the variation in dead volume (as in higher values of cubic capacities the curve is dislocated to the right), since compression ratio is being kept constant the variation in the displacement requires a proportional variation on dead volume. The pressure drop at the maximum cubic capacity can be explained by the long stroke, which reduces volumetric efficiency.

Figure (18) shows the influence of the variation of cubic capacity in the processes of intake and exhaust. It is perceived that pressure is kept almost constant at each process, except by the sensible pressure rise in exhaust and drop in intake, both explained by the relation that exists between the differential of pressure and rate of volume variation (Eq. (10)). As consequence, pressure can present a small drop during intake process, and as the mass flow depends on the ratio of pressure between in-cylinder pressure and manifold pressure (Eq. (9)), it is expected a light drop in volumetric efficiency at the maximum cubic capacity, as illustrated by Fig. (17).

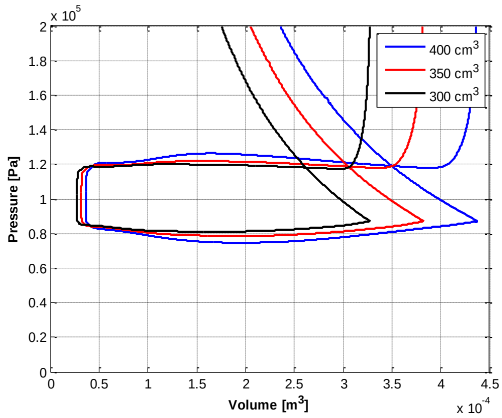

Figure 18. Detail of the open processes on the P-V diagram for variation cubic capacity

To perform a comparison of performance between the two strategies, it was verified that a variation from 80% to 100% of load at a cubic capacity of 400 cm³ is equivalent to vary the cubic capacity from 300 cm³ to 400 cm³ at full load, obtaining an equivalent power output, as shown by Fig. (19). In both cases, compression ratio was kept constant at 12:1.

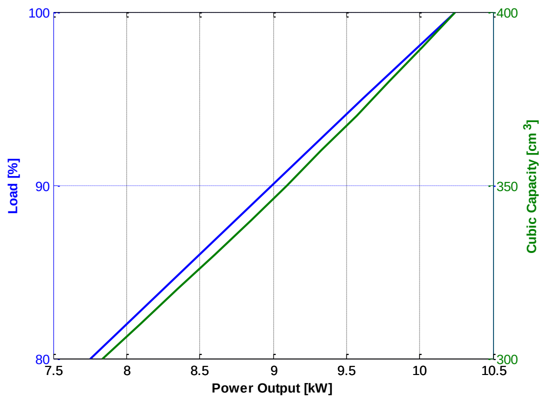

Figure 19. Comparison of the developed power by varying each load and cubic capacity.

Figure (20) illustrates the main difference between both strategies. As mentioned before, mean effective power is an indicative of power density. If cubic capacity is constant, it is necessary to reduce this "density" to limit the power output, while if cubic capacity could be adjusted, power would be limited by the amount of cubic capacity with a constant "density" of power. It is verified in Fig. (20), where **IMEP** is linearly proportional to power (Eq. (15)) in the variation of load because $\mathbf{W_{Cycle}}$ is being reduced while $\mathbf{V_{max}}$ is kept constant. When cubic capacity is reduced, $\mathbf{W_{Cycle}}$ and $\mathbf{V_{max}}$ are reduced together, yet at a different rate (as mentioned before, at reduced cubic capacities is possible to obtain a higher volumetric efficiency, as shown by Fig. (21)).

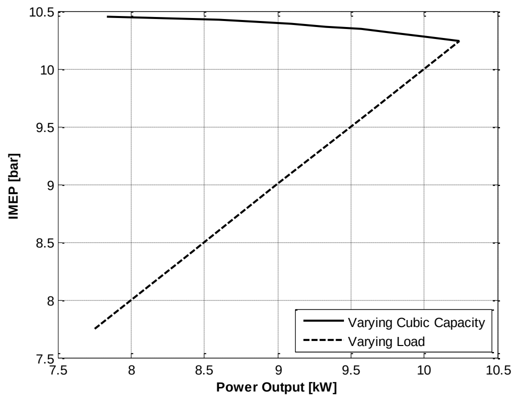

Figure 20. IMEP by indicated power.

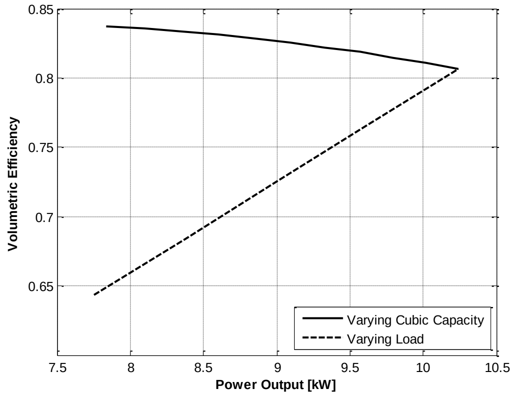

Figure 21. Volumetric efficiency by indicated power.

Although the volumetric efficiency is increased when the cubic capacity is reduced, the thermal efficiency presents a small drop (compared to the variation on load), explained by the losses due to the increased area/volume relation.

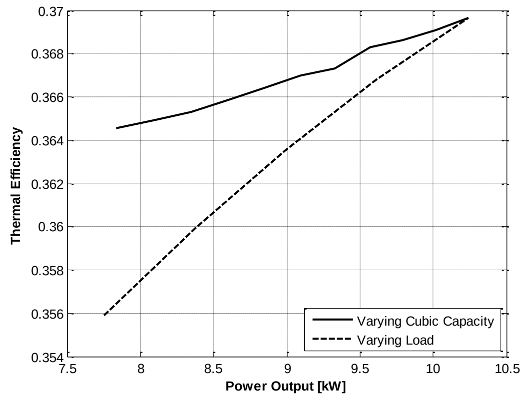

Figure 22. Thermal efficiency by indicated power.

The result presented in Figure (23) proves the direct relation between thermal efficiency and fuel consumption and illustrate how the technology proposed has a potential to reduce fuel consumption and therefore reduce emissions of pollutant.

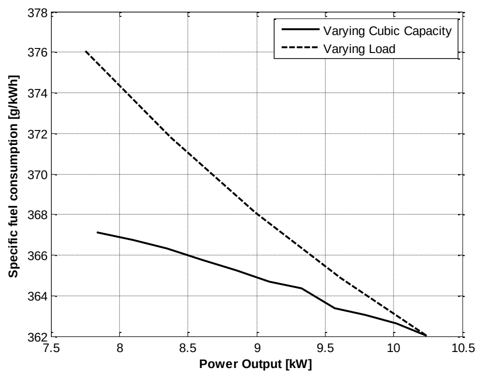

Figure 23. Specific fuel consumption by indicated power.

CONCLUSIONS

In this work it was explored the strategy of adjusting compression ratio and cubic capacity by proposing a mechanism which allows those adjustments. The described study has as objective the exposing of advantages obtained with the implementation of such technology for efficiency increase due to the flexibility that the mechanism would give to the engine, being this characteristic relative to the operational environment or nature of the fuel.

The authors do not expect that the adjustment of the cubic capacity is solely sufficient to cover an entire range of power which is required by the engine, so the throttle valve would be necessary for reduced loads, justifying the control over compression ratio. Therefore, when the engine operates near its minimum power (idle), cubic capacity will be at its minimum value and also the throttle will be restraining the air flow to intake manifold, however, it is noted that this restriction will be less than in a conventional engine and also, the loss of efficiency due to additional pump work will be compensated by the possible increase in compression ratio, since there would not be a risk of the knock occurrence.

This study characterizes itself in a preliminary study whose objective is to present and justify a new proposal for variable compression ratio and cubic capacity engine and the authors highlight the advantages that can already be observed. One must note that the spark time was kept constant, the engine was analysed only when the throttle operation was not necessary and the effects of varying cubic capacity and compression ratio were analysed separately. Future work include analysis of those parameters varying at the same time, what brings up the need of a strategy of calibration and also the need of a knock prediction model. Only then it will be possible to understand the full potential of this new technology as an alternative for the development of internal combustion engines.

ACKNOWLEDGEMENTS

The authors would like to express their gratitude to the institutions which supported the research by offering financial and technical resources: Fundação de Amparo à Pesquisa do Estado de São Paulo (FAPESP) and to the group PSA-Peugeot Citroën.

REFERENCES

1. MacLean, H. L. and Lave, L. B. Evaluating automobile fuel/propulsion system technologies. Progress in Energy and Combustion Science, 29:1-69, 2003.
2. Suarez-Bertoa, R., Mendoza-Villafuerte, P., Bonnel, P., et al. On-road measurement of nh 3 and n 2 o emissions from a euro v heavy-duty vehicle. Atmospheric Environment, 139:167-175, 2016.
3. Szwarcfiter, L., Mendes, F. E., and La Rovere, E. L. Enhancing the efects of the brazilian program to reduce atmospheric pollutant emissions from vehicles. Transportation Research Part D: Transport and Environment, 10(2):153-160, 2005.
4. Brazil. Decreto no 7,819, de 3 de outubro de 2012. Regulamenta os arts. 40 a 44 da Lei No 12.715, de 17 de setembro de 2012, que dispõe sobre o Programa de Incentivo à Inovação Tecnológica e Adensamento da Cadeia Produtiva de Veículos Automotores - INOVARAUTO, e os arts. 5o e 6o da Lei No 12.546, de 14 de dezembro de 2011, que dispõe sobre redução do Imposto sobre Produtos Industrializados, na hipótese que especifica. Diário Oficial, Brasília, DF, 03/10/2012.
5. Bandivadekar, A. On the road in 2035: reducing transportation's petroleum consumption and GHG emissions. Massachusetts Institute of Technology, 2008.
6. de Melo, T. C. C., Machado, G. B., Belchior, C. R., et al. Hydrous ethanol-gasoline blends-combustion and emission investigations on a ex-fuel engine. Fuel, 97:796-804, 2012.
7. Roberts, M. Benefits and challenges of variable compression ratio (vcr). SAE Technical Paper No 2003-01-0398, 2003.
8. Shaik, A., Moorthi, N. V., and Rundramoorthy, R. Variable compression ratio engine: a future power plant for automobiles - an overview. Proc. IMechE Part D: Automobile Engineering, 221, 2007.
9. Adams, W. H., Hinrichs, H. G., Pischinger, F. F., et al. Analysis of the combustion process of a spark ignition engine with a variable compression ratio. SAE Technical Paper No 870610, 1987.
10. Drangel, H., Olofsson, E., and Reinmann, R. The variable compression (svc) and the combustion control (scc)-two ways to improve fuel economy and still comply with world-wide emission requirements. SAE Technical paper No 2002-01-0996, 2002.
11. Wittek, K., Tiemann, C., and Pischinger, S. Two-stage variable compression ratio with eccentric piston pin and exploitation of crank forces. SAE Technical Paper No 2009-01-1457, 2009.
12. Wirbeleit, F. G., Binder, K., and Gwinner, D. Development of pistons with variable compression height for increasing efficiency and specic power output of combustion engines. SAE Technical Paper No 900229,1990.
13. Cassiani, M. B. Análise cinemática e dinâmica de mecanismos de motores de taxa de

compressão variável. Master's thesis, School of Mechanical Engineering, University of Campinas, 2011.
14. Alsterfalk, M., Filipi, Z. S., e Assanis, N. The potential of the variable stroke spark-ignition engine. SAE Technical Paper No 970067, 1997.
15. Siewert, R. Engine combustion at large bore-to-stroke ratios. SAE Technical Paper No 780968, 1978.
16. Pouliot, H. N., Delameter, W. R., and Robinson, C. W. A variable displacement spark ignition engine. SAE Technical Paper No 770114, 1977.
17. P. A. Rosso, J. B. e Blough, J. R. A variable displacement engine with independently controllable stroke length and compression ratio. SAE Technical Paper No 2006-01-0741, 2006.
18. Yamin, J. A. and Dado, M. H. Performance simulation of a four-stroke engine with variable stroke-length and compression ratio. Applied energy, 77(4):447-463, 2004.
19. Beroff, J. Internal combustion engine with variable capacity and compression ratio, 2000. Patente, deposit European Patent Office No EP 1 143 127 B1.
20. Ferreira, J. V. e Rufino, C. H. Motor de combustão interna com mecanismo que permite controle instantâneo sobre a taxa de compressão e a capacidade volumétrica de cada cilindro individualmente e seus usos, 2014. Patent, deposit INPI No BR 10 2014 026240 7.
21. Stull, D. and Prophet, H. Janaf thermochemical tables. Technical report, DTIC Document, 1971.
22. Lanzafame, R. Water injection effects in a single cylinder cfr engine. SAE Technical Paper No 1999-01-0568, 1999.
23. Alla, A. Computer simulation of a four stroke spark ignition engine. Energy Conversion and Management, 43:1043-1061, 2002.
24. Hohenberg, G. F. Advanced approaches for heat transfer calculations. SAE Technical Paper No 790825, 1979.
25. Nishiwaki, K., Shimamoto, Y., and Miyake, K. Average heat transfer coefficients on a cylinder wall in the intake and exhaust processes of motoring test. Bulletin of JSME, 22(174):1796-1809, 1979.
26. Kastner, L., Williams, T., White, J., et al. Poppet inlet valve characteristics and their influence on the induction process. Proceedings of the Institution of Mechanical Engineers, 178(1):955-975, 1963.
27. Gallo, W. Análise Exergética de Motores a Gasolina e a Álcool. PhD's thesis, School of Mechanical Engineering, University of Campinas, 1990.
28. Zacharias, F. Analytical representation of the thermodynamic properties of combustion gases. SAE Technical Paper No 670930, 1967.
29. Lopes, A. V. B. Simulação fenomenológica de motores diesel. Master's thesis, School of Mechanical Engineering, University of Campinas, 2014.